Main-Group Complexes

International Edition: DOI: 10.1002/anie.201907749
German Edition: DOI: 10.1002/ange.201907749

A Neutral "Aluminocene" Sandwich Complex: η^1- versus η^5-Coordination Modes of a Pentaarylborole with ECp* (E = Al, Ga; Cp* = C_5Me_5)

Christian P. Sindlinger and Paul Niklas Ruth*

Abstract: *The pentaaryl borole (Ph*C)$_4$BXyl^F [Ph* = 3,5-$tBu_2(C_6H_3)$; Xyl^F = 3,5-$(CF_3)_2(C_6H_3)$] reacts with low-valent Group 13 precursors AlCp* and GaCp* by two divergent routes. In the case of [AlCp*]$_4$, the borole reacts as an oxidising agent and accepts two electrons. Structural, spectroscopic, and computational analysis of the resulting unprecedented neutral η^5-Cp*,η^5-[(Ph*C)$_4$BXyl^F] complex of Al^{III} revealed a strong, ionic bonding interaction. The formation of the heteroleptic borole-cyclopentadienyl "aluminocene" leads to significant changes in the ^{13}C NMR chemical shifts within the borole unit. In the case of the less-reductive GaCp*, borole (Ph*C)$_4$BXyl^F reacts as a Lewis acid to form a dynamic adduct with a dative 2-center-2-electron Ga–B bond. The Lewis adduct was also studied structurally, spectroscopically, and computationally.*

Fifty years ago, Eisch reported the first authentic isolation of pentaphenyl borole.[1] Free boroles are weakly anti-aromatic cyclic 4π-electron compounds.[2] Among a variety of intriguing reactivities, including the activation of hydrogen[3] or Si–H bonds,[4] Diels–Alder reactions, and ring expansions,[1b,5] boroles can be readily reduced by two electrons to form Hückel-aromatic boroledііdes[6] or they can react as potent Lewis acids.[7] In recent years, variation of the boron-bound substituent allowed for an extension of the library of known boroles with substantially altered optical gaps.[2b,6b,8]

The coordination chemistry of boroles toward transition metals has been studied since the late 1970s.[6a,9] However, despite the isoelectronic nature of boroledііde with the—in organometallic chemistry—ubiquitous and iconic cyclopentadienyl anion, very few complexes other than with d-block metals or very electron-positive s-block metals are known. Recently Müller, Albers, and co-workers reported a Ge^{II}-borole complex that resulted from a rearrangement during the reaction of a germole dianion with amidoborane dihalides.[10] Although only a few comments are found in the literature,[9d,11] a likely reason for the scarcity of p-block complexes, in particular, is that boroledііde salts act as reducing agents rather than as a ligand source in metathesis reactions with p-block halides.

We recently reported the synthesis of a set of novel, highly soluble *tert*-butyl-decorated pentaphenyl boroles (Ph*C)$_4$BR [Ph* = 3,5-$tBu_2(C_6H_3)$].[12] We are interested in further expanding the chemical scope of boroles as ligands to the p-block elements. To circumvent salt metathesis reactions, we treated borole (Ph*C)$_4$BXyl^F (**A**) with the established, potentially reductive monovalent Group 13 reagents (AlCp*)$_4$ and GaCp* (Scheme 1).

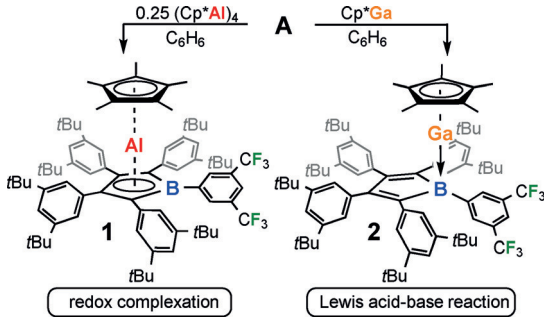

Scheme 1. Divergent reaction pathways of free borole **A** with AlCp* and GaCp*.

When GaCp* was added to borole **A** an immediate colour change from dark green to bright orange was observed. NMR spectroscopic examination of the reaction mixture confirmed a clean conversion and the formation of a single product. The ^{1}H NMR spectrum revealed no substantial changes in the shifts compared to the individual starting materials. However, the ^{11}B NMR signal drastically shifts from a broad signal in the typical range of tricoordinate boron atoms at δ_{11B} = 71 ppm ($\omega_{1/2}$ = ca. 3250 Hz) in **A** to a narrower signal at δ_{11B} = 7.6 ppm ($\omega_{1/2}$ = ca. 1550 Hz) in **2**. The shift to higher field is a clear indication of a higher coordination number at the boron atom.[13] Major changes ($\geq \pm 2$ ppm) in the ^{13}C{^{1}H} NMR spectrum of the borole framework are observed for the α- and β-carbon atoms of the C_4B cycle as well as the *ipso*- and *para*-positions of the boron-bound aryl moiety (Table 1).

An interaction of the GaCp* fragment with the boron-centred LUMO is also in line with the change in colour from an intense green (stemming from π/π* excitation in free boroles) to a bright orange. The colour of **2** is unique among the otherwise colorless (Cp/R)Ga^I adducts with Lewis-acidic boranes.[13,14]

[*] Dr. C. P. Sindlinger, M.Sc. P. N. Ruth
Institut für Anorganische Chemie
Georg-August-Universität Göttingen
Tammannstrasse 4, 37077 Göttingen (Germany)
E-mail: christian.sindlinger@chemie.uni-goettingen.de

Supporting information (including Experimental Details) and the ORCID identification number for one of the authors of this article can be found under: https://doi.org/10.1002/anie.201907749.

Table 1: Diagnostic NMR chemical shifts in C_6D_6 at 298 K of **A**, **1**, and **2**. Calculated averaged values in brackets.

Compound	C_β[b]	C_α[b]	*i*-C_{XylF}[b]	*p*-C_{XylF}[b]	^{11}B
A[a]	166.2	140.6	135.9	125.3	71.6
1	128.4	118.0	144.2	119.1	24.6/17.3[c]
	[126.1]	[117.9]	[144.8]		[18.6]
2	151.2	149.6	150.7	119.4	7.6/−0.4[d]
	[151.7]	[149.9]	[151.6]		[−0.9]

[a] See Ref. [12]. [b] ^{13}C NMR shift in ppm in C_6D_6. [c] At −75 °C in toluene. [d] At −50 °C in toluene.

At ambient temperature, no further signal for free GaCp* was observed after addition of a further 0.5 equiv of GaCp* to solutions of **2**, thus indicating a dynamic exchange of GaCp*. Variable-temperature NMR experiments of solutions of **2** in toluene with a slight excess of GaCp* reveal hindered rotation of the C_β-bound Ph* groups starting at −40 °C. At −30 °C, the Cp* signal significantly broadens and gradual cooling from −40 °C to −75 °C leads to two increasingly sharp separate Cp* signals of GaCp* and **2** being observed. The ^1H NMR chemical shifts all lie in the range of pure GaCp*, which is reported to likely form hexamers at low temperature.[15] However, the intense orange colour does not change upon cooling, thus rendering a potential equilibrium between **2** and **A** + 1/6 $[GaCp^*]_6$ unlikely. Orange-red crystals suitable for X-ray diffraction grew from benzene solutions. The molecular structure clearly confirms the formation of a boron-centred Lewis-base adduct, with donation of the Ga^I lone pair of electrons into an empty p orbital on boron (Figure 1). The Ga1–$Cp^*_{centroid}$ vector is virtually aligned with the Ga1–B1 bond (175.5°), and the Ga1–B1 vector is almost perpendicular to the C_4B plane (C4-B1-Ga1 95.04(11)°, C1-B1-Ga1 92.60(11)°. The Ga–B bond (2.1382(19) Å) is similar to those in $B(C_6F_5)_3$ adducts of GaCp derivatives (2.154(3), 2.155(6), 2.161(2) Å).[13a,14b] The bond lengths within the borole ring clearly reveal isolated C=C and C–C bonds. The Xyl^F residue at the tetracoordinate boron centre noticeably bends out of the borole plane away from the GaCp* cone. A related structural motif and reactivity was also observed for AlCp* adducts of 9-borafluorenes.[11]

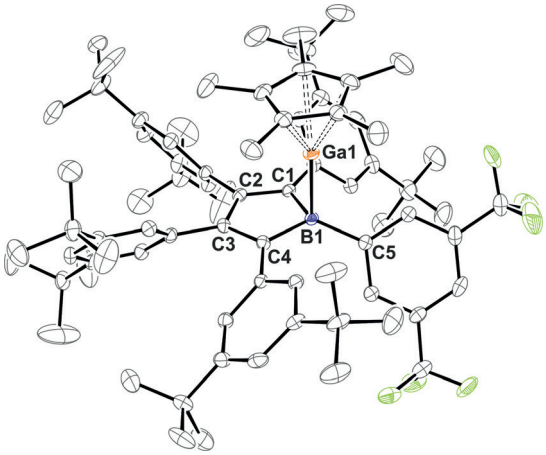

Figure 1. ORTEP plot of the molecular structure of the Lewis acid-base complex (**A**·GaCp*) (**2**).[26] Atomic displacement parameters are drawn at the 50% probability level. Hydrogen atoms, disordered *t*-Bu groups, and a lattice benzene molecule have been omitted for the sake of clarity. Selected bond lengths [Å] and angles [°] are given: Ga1-B1 2.1382(19), B1-C5 1.599(3), B1-C1 1.604(3), B1-C4 1.600(3), C1-C2 1.370(2), C2-C3 1.471(2), C3-C4 1.377(2), Ga1-Cp* 2.2152(18), 2.2355(19), 2.2579(18), 2.2754(19), 2.2973(19), Ga1-$Cp^*_{centroid}$ 1.902; C5-B1-Ga1 109.28(12), C4-B1-Ga1 95.04(11), C1-B1-Ga1 92.60(11), B1-Ga1-$Cp^*_{centroid}$ 175.5.

Over the course of a few weeks, small amounts of a fine grey solid deposited from solutions of **2** along with the formation of unassigned decomposition products.[15]

Clearly, the monovalent Ga^ICp^* was too reluctant to transfer electrons and reduce the borole. We therefore turned to $(AlCp^*)_4$, as Al^I is a stronger reductant. AlCp derivatives can also form base adducts with boranes.[16] Suspending the poorly soluble $(AlCp^*)_4$ in green solutions of **A** leads to a very slow decolourisation over the course of three days to finally yield pale yellow solutions. Monitoring the process by NMR spectroscopy revealed a very clean conversion into a single product **1**. Crystals of **1** readily form from concentrated solutions in various hydrocarbons. In all cases, and despite numerous attempts, we obtained poorly resolved diffraction data.[17] Examination of the data, however, allowed the key structural feature to be clearly identified: the anticipated quasi η^5-Cp*,η^5-$[(Ph^*C)_4BXyl^F]$ Al^{III} sandwich complex **1**. This represents the first neutral "aluminocene" and the second borole complex of a p-block element.[10,18] Heteroleptic Cp/borole sandwich complexes are known for various transition metals.[8e,19]

The quality of the data limits extensive structural discussion; however, some key features can clearly be identified. Compared to **A** and **2**, which both feature localized cyclic 1,3-butadiene systems, the atomic distances within the (C_4B) ring in **1** are much more uniform. Shortened B–C_α and C_β–C_β bonds together with an elongated C_α–C_β bond are in line with substantial π-delocalization, as expected for a Hückel-aromatic boroldiide.[6b] The Al1-$(C_4B)_{centroid}$ distance is approximately 1.80 Å, which is slightly shorter than the Al1-$Cp^*_{centroid}$ distance of approximately 1.86 Å. This is rationalized by greater electrostatic attraction between the dianionic borole and Al^{III} compared to the simple monoanionic Cp*. The Cp* and borole units adopt a distorted staggered conformation. The Cp*-Al contacts range from 2.17(1) to 2.27(1) Å, thus indicating a slight deviation of the Al atom from an ideal central localisation. The disorder in the X-ray structure prevents discussion of individual Al1–(C_4B) distances. The DFT-optimised structure (Figure 2) reveals a centered Al atom with comparatively short Al–C_α and Al–B contacts. All other experimental structural features are in general good agreement with the gas-phase DFT-optimised structure.[20]

Complex **1** reveals a ^{11}B NMR signal at $\delta_{11B} = 24.6$ ppm, shifted upfield from **A** but less so than **2**. A very broad ^{27}Al NMR resonance was observed at $\delta_{27Al} = -86.2$ ppm ($\omega_{1/2}$ = ca. 2600 Hz). Both shifts are in good agreement with those predicted computationally for the optimised gas-phase structure of $\delta = 18.6$ ppm (^{11}B) and $\delta = -90.0$ (^{27}Al).[21] The broad ^{27}Al resonance is different from the sharp signals in aluminocenium cations and is likely caused by a lower

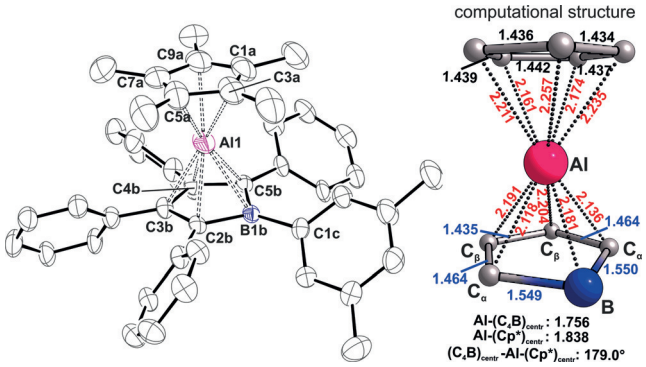

Figure 2. ORTEP plot (left)[26] and excerpt from the gas-phase DFT-optimised[20] molecular structure of the Al^{III} sandwich complex **1**. Atomic displacement parameters are drawn at the 40% probability level. Hydrogen and fluorine atoms, *t*Bu groups, and a disorder of ca. 50% occupation of the borole subunit have been omitted for the sake of clarity. Selected bond lengths [Å] and angles [°] are given. Disorder fraction given in parentheses: B1b-C2b 1.54(2)[1.54(2)], C2b-C3b 1.47(2)[1.46(2)], C3b-C4b 1.41(2)[1.42(2)], C4b-C5b 1.47(2)-[1.47(2)], C5b-B1b 1.53(2)[1.53(2)], B1b-C1c 1.59(2)[1.59(1)], B1b-Al1 2.14(2)[2.31(2)], C2b-Al1 2.22(1)[2.25(1)], C3b-Al1 2.32(1)[2.19(2)], C4b-Al1 2.17(1)[2.12(2)], C5b-Al1 2.00(1)[2.10(2)], Al1-C3a 2.27(1), Al1-C5a 2.22(1), Al1-C7a 2.17(1), Al1-C9a 2.18(1), Al1-C1a 2.24(1); $(C_4B)_{centroid}$-Al1 1.77[1.80], $Cp^*_{centroid}$-Al1 1.86; $(C_4B)_{centroid}$-Al1- $Cp^*_{centroid}$ 175.6[174.8].

symmetry and the quadrupole moments of the boron nuclei. The ^{27}Al chemical shift of **1** lies in-between those of half-sandwich complexes, such as $(AlCp^*)_4$ ($\delta = -78.3$ ppm),[22] $(AlCp^*)$-η^1-9-Ph-9-borafluorenes ($\delta = -70.3$ ppm),[11] or $AlCp^*$-$B(C_6F_5)_3$ ($\delta = -59.3$ ppm),[16a] and its closest structural relatives $[Cp^*_2Al]^+$ ($\delta = -102.9$ ppm), $[Cp'_2Al]^+$ ($\delta = -113$ ppm; $Cp' = Me_4C_5H$), and $[Cp_2Al]^+$ ($\delta = -126.4$ ppm).[23] The upfield shift in cationic aluminocenes has been associated with the aromatic nature of the $[Cp]^-$ ligands.[23a] The observed ^{27}Al shift for **1** is, therefore, in line with a less pronounced aromaticity of boroledиides. The symmetric ^1H NMR spectrum of **1** recorded in toluene at room temperature barely differs from the spectrum of free borole **A**, which indicates little hindrance of Ph* rotations around the Ph*–$C_{\alpha/\beta}$ bond. However, cooling readily leads to significant broadening of the *o*-Ph* signals in both the α- and β-positions. At −15 °C, these signals are broadened beyond recognition and at −75 °C up to eight individual signals for the *o*-Ph* protons and *t*Bu groups are present, along with a single broad Cp* resonance. This can be rationalized by a static borole subunit structure much like that observed in the solid state with totally locked Ph*-$C_{\alpha/\beta}$ rotations that even suppress a switching between the tilt conformation of the borole paddlewheel. This low-temperature behaviour is significantly different from **2** and strongly supports the η^5-(borole) coordination mode being maintained in cool solutions.

The two fundamentally different reaction pathways of borole **A** with GaCp* and AlCp* also become apparent in diagnostic ^{13}C chemical shifts of the C_α- and C_β-carbon atoms of C_4B (Table 1). Two-electron reduction and complexation to form compound **1** results in the rather low-field-resonating signals observed in free borole **A** drastically shifting to a higher field by 37.8 ppm (C_β) and 22.6 ppm (C_α). Their assignment is supported by excellent agreement with the computationally predicted shifts. This field range is commonly observed for cyclopentadienyl resonances of ECp derivatives. The excellent agreement of the δ_{calc} and δ_{exp} values also further corroborates the η^5-type coordination mode of the borole to be present both in the solid state as well as in solution.

In the case of base adduct **2**, only C_β is shifted to a higher field, whereas C_α resonates at an even lower field than in **A**. Interestingly, both fundamentally different reactions cause the *p*-Xyl^F resonance to shift to a slightly higher field, which is more typical for *p*-aryl groups. This is likely due to the population of the empty p-orbital on boron and prevention of mesomeric delocalization of a positive charge through the π-system into the boron-bound aryl group.

Compounds **1** and **2** were also investigated by mass spectrometry using a LIFDI set-up.[24] Whereas **1** revealed clean spectra of only $[M(\mathbf{1})]^+$, concentrated solutions of **2** in toluene under identical conditions revealed only $[M(\mathbf{A}+H_2O)]^+$ and, to a lesser extent, $[M(\mathbf{A})]^+$. This is surprising as we never observe $[M(\mathbf{A})]^+$ in pure solutions of **A**, which always revealed clean $[M(\mathbf{A}+H_2O)]^+$ signals.

Computational probing of the complexes **1** and **2** allows further insight into the electronic structure of the two different interactions modes of borole $(Ph^*C)_4BXyl^F$ (**A**) with ECp* (E = Al, Ga). The computational (BP86-D3/def2-TZVP) free dissociation energy to form free **A** and ECp* is substantially higher for **1** (39.4 kcal mol^{-1}) than for **2** (12.8 kcal mol^{-1}).

The successful transfer of two electrons onto the borole ring in **1** becomes apparent from the borole-based HOMO essentially being identical with the LUMO in free **A** (Figure 3). LUMO + 2 is Al-based with high s-character. This is further in line with a Bader charge of + 2.29 at Al. The borole (C_4B) unit accumulates a Bader charge of −0.78. However, this charge resides on the butadiene backbone (C_β −0.24; C_α −0.99; B +1.68). As expected, the charge accumulated on the central (C_5)-Cp* moiety amounting to −1.17 is equally distributed between the five carbon atoms. A QTAIM topology analysis revealed no bond critical point on the Al-B vector; however, ring and cage critical points are found (Figure 4). In line with a strong localisation of electron density on C_α, bond critical points are only found for the Al-C_α vectors (delocalization index, DI = 0.25) but not for the Al-C_β contact (DI = 0.11).[25] The analysis of the hypothetical model complex $(C_4BH_5)Al(C_5H_5)$[11] revealed identical features. Müller, Albers, and co-workers also found no Ge–B bonding path in their Ge^{II} aminoborole complex.[10] Similar Wiberg bond indices (WBI) for all the Al-(C_4B) contacts support the η^5-coordination mode of the borole (Scheme 2a). A comparatively high WBI for the C_β–C_β bond is in line with the putatively dominating resonance structure **IV**, which also corroborates the QTAIM charge localization on C_α. A natural resonance theory (NRT) calculation on the isolated $[C_4BH_5]^{2-}$ dianion provides a contribution weighting of resonance structures **I–III. IV** is not proposed by NRT, but can be directly derived from **II**. The accumulation of dianionic charge on the C_α–B–C_α moiety (**II** and **III**) accounts for the

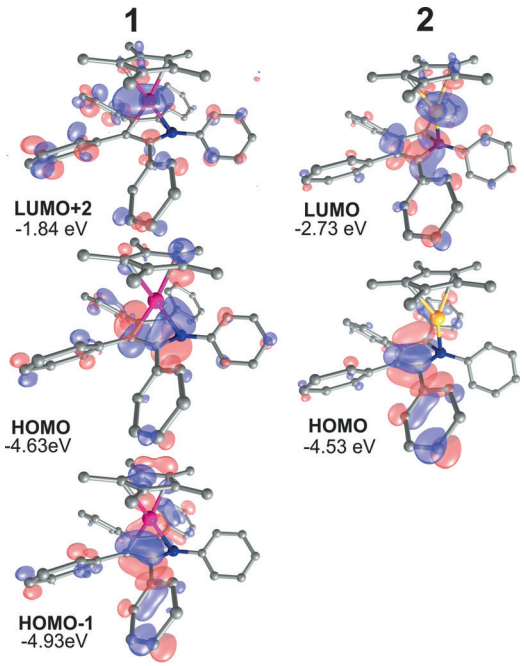

Figure 3. Frontier orbital depictions of molecules **1** and **2**.[20] *t*Bu and CF_3 groups are omitted for clarity. Isosurfaces are shown at 0.04 a.u.

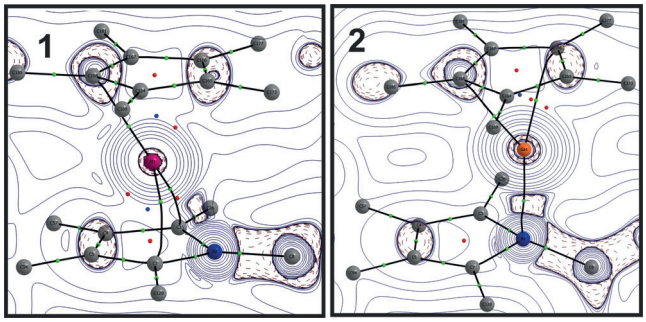

Figure 4. Excerpts of the molecular graph and contour plots of the Laplacian of the electron density ($\nabla^2\rho(r)$) isosurfaces through the E-B-$(C_\beta\text{-}C_\beta)_{centroid}$ planes of molecules **1** (left) and **2** (right). Maroon dotted lines: negative Laplacian (area of charge concentration), blue solid lines: positive Laplacian (area of charge depletion), green dots: bond critical points, red dots: ring critical points, blue dots: cage critical points.[20]

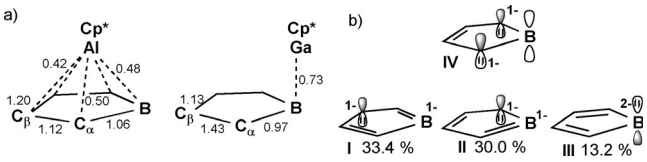

Scheme 2. a) WBI for **1** and **2**.[20] b) Selection of mesomeric descriptions of $[C_4B]^{2-}$ that putatively contribute to the structure of **1.** The weightings of resonance structures **I–III** were obtained from NRT calculations on isolated $[C_4BH_5]^{2-}$, with **IV** being a putative dominant resonance structure of **1**.

relatively short B–Al distances observed for the structures of all the computationally probed (C_4B)AlCp derivatives (Scheme 2b).

The HOMO and LUMO in gallium(I) adduct **2** still greatly resemble those in free borole **A**, with the LUMO revealing strong contributions of the GaCp* fragment. The dative Ga–B bond is instead delocalized over several lower lying MOs. A bond critical point was found on the Ga-B vector and a Bader charge of +0.79 was calculated for Ga. The borole (C_4B) unit is almost neutral with a combined Bader charge of +0.32 versus an anionic Cp* (C_5) moiety (−0.73).

In summary, we have presented two divergent routes of a weakly anti-aromatic and Lewis-acidic pentaarylborole with monovalent Group 13 cyclopentadienyl compounds, namely AlCp* and GaCp*. Depending on the energetic accessibility of their two lone pairs of electrons, we observed either redox chemistry to form a neutral heteroleptic boroldiide/cyclopentadienyl "aluminocene" or formation of a Lewis-base adduct with a dative Ga–B bond. These observations on the stability and bonding interactions of p-block complexes of boroles with electropositive p-block metals improve the understanding of the general applicability of boroles in coordination chemistry.

Acknowledgements

We are indebted to the Fonds der Chemischen Industrie for a Liebig fellowship. Prof. Dietmar Stalke is acknowledged for supportive and generous mentorship. This work was funded by the Deutsche Forschungsgemeinschaft (DFG, German Research Foundation) grant 389479699/GRK2455 (PhD grant to P.N.R.).

Conflict of interest

The authors declare no conflict of interest.

Keywords: aluminocenes · aromaticity · boroles · Group 13 elements · main group complexes

How to cite: *Angew. Chem. Int. Ed.* **2019**, *58*, 15051–15056
Angew. Chem. **2019**, *131*, 15193–15198

[1] a) J. J. Eisch, N. K. Hota, S. Kozima, *J. Am. Chem. Soc.* **1969**, *91*, 4575–4577; b) J. J. Eisch, J. E. Galle, S. Kozima, *J. Am. Chem. Soc.* **1986**, *108*, 379–385.

[2] a) H. Braunschweig, I. Fernández, G. Frenking, T. Kupfer, *Angew. Chem. Int. Ed.* **2008**, *47*, 1951–1954; *Angew. Chem.* **2008**, *120*, 1977–1980; b) J. Köhler, S. Lindenmeier, I. Fischer, H. Braunschweig, T. Kupfer, D. Gamon, C.-W. Chiu, *J. Raman Spectrosc.* **2010**, *41*, 636–641; c) H. Braunschweig, I. Krummenacher, J. Wahler, in *Advances in Organometallic Chemistry*, *Vol. 61* (Eds.: A. F. Hill, M. J. Fink), Academic Press, San Diego, **2013**, pp. 1–53; d) J. O. C. Jimenez-Halla, E. Matito, M. Sola, H. Braunschweig, C. Horl, I. Krummenacher, J. Wahler, *Dalton Trans.* **2015**, *44*, 6740–6747.

[3] C. Fan, L. G. Mercier, W. E. Piers, H. M. Tuononen, M. Parvez, *J. Am. Chem. Soc.* **2010**, *132*, 9604–9606.

[4] H. Braunschweig, A. Damme, C. Hörl, T. Kupfer, J. Wahler, *Organometallics* **2013**, *32*, 6800–6803.

[5] a) J. J. Eisch, J. E. Galle, *J. Am. Chem. Soc.* **1975**, *97*, 4436 – 4437; b) S. A. Couchman, T. K. Thompson, D. J. D. Wilson, J. L. Dutton, C. D. Martin, *Chem. Commun.* **2014**, *50*, 11724 – 11726; c) H. Braunschweig, C. Hörl, L. Mailänder, K. Radacki, J. Wahler, *Chem. Eur. J.* **2014**, *20*, 9858 – 9861; d) J. H. Barnard, P. A. Brown, K. L. Shuford, C. D. Martin, *Angew. Chem. Int. Ed.* **2015**, *54*, 12083 – 12086; *Angew. Chem.* **2015**, *127*, 12251 – 12254; e) K. Huang, C. D. Martin, *Inorg. Chem.* **2015**, *54*, 1869 – 1875; f) H. Braunschweig, I. Krummenacher, L. Mailänder, F. Rauch, *Chem. Commun.* **2015**, *51*, 14513 – 14515; g) H. Braunschweig, F. Hupp, I. Krummenacher, L. Mailänder, F. Rauch, *Chem. Eur. J.* **2015**, *21*, 17844 – 17849; h) H. Braunschweig, M. A. Celik, F. Hupp, I. Krummenacher, L. Mailänder, *Angew. Chem. Int. Ed.* **2015**, *54*, 6347 – 6351; *Angew. Chem.* **2015**, *127*, 6445 – 6449; i) J. H. Barnard, S. Yruegas, K. Huang, C. D. Martin, *Chem. Commun.* **2016**, *52*, 9985 – 9991; j) S. Yruegas, D. C. Patterson, C. D. Martin, *Chem. Commun.* **2016**, *52*, 6658 – 6661; k) K. Huang, C. D. Martin, *Inorg. Chem.* **2016**, *55*, 330 – 337; l) J. H. Barnard, S. Yruegas, S. A. Couchman, D. J. D. Wilson, J. L. Dutton, C. D. Martin, *Organometallics* **2016**, *35*, 929 – 931; m) V. A. K. Adiraju, C. D. Martin, *Chem. Eur. J.* **2017**, *23*, 11437 – 11444; n) J. J. Baker, K. H. M. Al-Furaiji, O. T. Liyanage, D. J. D. Wilson, J. L. Dutton, C. D. Martin, *Chem. Eur. J.* **2019**, *25*, 1581 – 1587; o) F. Lindl, S. Lin, I. Krummenacher, C. Lenczyk, A. Stoy, M. Müller, Z. Lin, H. Braunschweig, *Angew. Chem. Int. Ed.* **2019**, *58*, 338 – 342; *Angew. Chem.* **2019**, *131*, 344 – 348.

[6] a) G. E. Herberich, B. Buller, B. Hessner, W. Oschmann, *J. Organomet. Chem.* **1980**, *195*, 253 – 259; b) C.-W. So, D. Watanabe, A. Wakamiya, S. Yamaguchi, *Organometallics* **2008**, *27*, 3496 – 3501.

[7] A. Fukazawa, J. L. Dutton, C. Fan, L. G. Mercier, A. Y. Houghton, Q. Wu, W. E. Piers, M. Parvez, *Chem. Sci.* **2012**, *3*, 1814 – 1818.

[8] a) H. Braunschweig, T. Kupfer, *Chem. Commun.* **2008**, 4487 – 4489; b) H. Braunschweig, F. Breher, C.-W. Chiu, D. Gamon, D. Nied, K. Radacki, *Angew. Chem. Int. Ed.* **2010**, *49*, 8975 – 8978; *Angew. Chem.* **2010**, *122*, 9159 – 9162; c) H. Braunschweig, C.-W. Chiu, K. Radacki, P. Brenner, *Chem. Commun.* **2010**, *46*, 916 – 918; d) H. Braunschweig, V. Dyakonov, J. O. C. Jimenez-Halla, K. Kraft, I. Krummenacher, K. Radacki, A. Sperlich, J. Wahler, *Angew. Chem. Int. Ed.* **2012**, *51*, 2977 – 2980; *Angew. Chem.* **2012**, *124*, 3031 – 3034; e) H. Braunschweig, C.-W. Chiu, D. Gamon, M. Kaupp, I. Krummenacher, T. Kupfer, R. Müller, K. Radacki, *Chem. Eur. J.* **2012**, *18*, 11732 – 11746; f) H. Braunschweig, C.-W. Chiu, A. Damme, B. Engels, D. Gamon, C. Hörl, T. Kupfer, I. Krummenacher, K. Radacki, C. Walter, *Chem. Eur. J.* **2012**, *18*, 14292 – 14304; g) H. Braunschweig, A. Damme, J. O. C. Jimenez-Halla, C. Hörl, I. Krummenacher, T. Kupfer, L. Mailänder, K. Radacki, *J. Am. Chem. Soc.* **2012**, *134*, 20169 – 20177; h) Z. Zhang, R. M. Edkins, M. Haehnel, M. Wehner, A. Eichhorn, L. Mailänder, M. Meier, J. Brand, F. Brede, K. Müller-Buschbaum, H. Braunschweig, T. B. Marder, *Chem. Sci.* **2015**, *6*, 5922 – 5927.

[9] a) G. E. Herberich, J. Hengesbach, U. Kölle, G. Huttner, A. Frank, *Angew. Chem. Int. Ed. Engl.* **1976**, *15*, 433 – 434; *Angew. Chem.* **1976**, *88*, 450 – 451; b) G. E. Herberich, J. Hengesbach, U. Kölle, W. Oschmann, *Angew. Chem. Int. Ed. Engl.* **1977**, *16*, 42 – 43; *Angew. Chem.* **1977**, *89*, 43 – 44; c) G. E. Herberich, B. Hessner, W. Boveleth, H. Lüthe, R. Saive, L. Zelenka, *Angew. Chem. Int. Ed. Engl.* **1983**, *22*, 996; *Angew. Chem.* **1983**, *95*, 1024; d) G. E. Herberich, H. Ohst, *Chem. Ber.* **1985**, *118*, 4303 – 4313; e) G. E. Herberich, W. Boveleth, B. Hessner, D. P. J. Köffer, M. Negele, R. Saive, *J. Organomet. Chem.* **1986**, *308*, 153 – 166; f) G. E. Herberich, U. Englert, M. Hostalek, R. Laven, *Chem. Ber.* **1991**, *124*, 17 – 23; g) R. W. Quan, G. C. Bazan, W. P. Schaefer, J. E. Bercaw, A. F. Kiely, *J. Am. Chem. Soc.* **1994**, *116*, 4489 – 4490; h) C. K. Sperry, W. D. Cotter, R. A. Lee, R. J. Lachicotte, G. C. Bazan, *J. Am. Chem. Soc.* **1998**, *120*, 7791 – 7805; i) T. J. Woodman, M. Thornton-Pett, D. L. Hughes, M. Bochmann, *Organometallics* **2001**, *20*, 4080 – 4091.

[10] P. Tholen, Z. Dong, M. Schmidtmann, L. Albers, T. Müller, *Angew. Chem. Int. Ed.* **2018**, *57*, 13319 – 13324; *Angew. Chem.* **2018**, *130*, 13503 – 13508.

[11] P. E. Romero, W. E. Piers, S. A. Decker, D. Chau, T. K. Woo, M. Parvez, *Organometallics* **2003**, *22*, 1266 – 1274.

[12] T. Heitkemper, C. P. Sindlinger, *Chem. Eur. J.* **2019**, *25*, 6628 – 6637.

[13] a) N. J. Hardman, P. P. Power, J. D. Gorden, C. L. B. Macdonald, A. H. Cowley, *Chem. Commun.* **2001**, 1866 – 1867; b) N. J. Hardman, R. J. Wright, A. D. Phillips, P. P. Power, *J. Am. Chem. Soc.* **2003**, *125*, 2667 – 2679.

[14] a) P. Jutzi, B. Neumann, G. Reumann, L. O. Schebaum, H.-G. Stammler, *Organometallics* **2001**, *20*, 2854 – 2858; b) C. Schenk, R. Köppe, H. Schnöckel, A. Schnepf, *Eur. J. Inorg. Chem.* **2011**, 3681 – 3685.

[15] D. Loos, E. Baum, A. Ecker, H. Schnöckel, A. J. Downs, *Angew. Chem. Int. Ed. Engl.* **1997**, *36*, 860 – 862; *Angew. Chem.* **1997**, *109*, 894 – 896.

[16] a) J. D. Gorden, A. Voigt, C. L. B. Macdonald, J. S. Silverman, A. H. Cowley, *J. Am. Chem. Soc.* **2000**, *122*, 950 – 951; b) A. Hofmann, C. Pranckevicius, T. Tröster, H. Braunschweig, *Angew. Chem. Int. Ed.* **2019**, *58*, 3625 – 3629; *Angew. Chem.* **2019**, *131*, 3664 – 3668; c) A. Hofmann, M.-A. Légaré, L. Wüst, H. Braunschweig, *Angew. Chem. Int. Ed.* **2019**, *58*, 9776 – 9781; *Angew. Chem.* **2019**, *131*, 9878 – 9883.

[17] X-ray diffraction data sets obtained from various solvents and crystallisation were all of the same limited resolution. However, the observed structural features were very similar in each case. In addition to trivial disorder of the *t*Bu groups, the whole borole fragment is disordered along the molecules quasi-fivefold axis. Detection of reflexion data at resolutions smaller than 1.2 Å was not possible even with very long exposure times, because of the substantial amount of disorder. The systematic observation of the disorder along the quasi-fivefold axis of symmetry within the molecule itself is an argument for the presence of an η^5-coordination mode.

[18] A few reported tetracarba-*nido*-hexaborane(6) clusters which could be described as boron complexes of boroles are not considered here; see, for example: H. Braunschweig, S. Ghosh, J. O. C. Jimenez-Halla, J. H. Klein, C. Lambert, K. Radacki, A. Steffen, A. Vargas, J. Wahler, *Chem. Eur. J.* **2015**, *21*, 210 – 218.

[19] a) G. E. Herberich, J. Hengesbach, G. Huttner, A. Frank, U. Schubert, *J. Organomet. Chem.* **1983**, *246*, 141 – 149; b) D. A. Loginov, D. V. Muratov, P. V. Petrovskii, Z. A. Starikova, M. Corsini, F. Laschi, F. d. B. Fabrizi, P. Zanello, A. R. Kudinov, *Eur. J. Inorg. Chem.* **2005**, 1737 – 1746; c) M. Enders, H. Pritzkow, W. Siebert, *Chem. Ber.* **1992**, *125*, 1981 – 1985; d) F. E. Hong, C. W. Eigenbrot, T. P. Fehlner, *J. Am. Chem. Soc.* **1989**, *111*, 949 – 956.

[20] Calculations at the BP86-D3BJ/def2TZVP level of theory. Optimisations of the aluminium system starting from the observed η^5 X-ray structure as well as from the η^1 gallium structure, resulted in the same η^5-type gas-phase structure.

[21] NMR shifts were calculated using the GIAO method implemented in ORCA4.1 on the gas-phase structures without solvent models. For the ORCA program system, see a) F. Neese, *WIREs Comput. Mol. Sci.* **2012**, *2*, 73 – 78; b) F. Neese, *WIREs Comput. Mol. Sci.* **2018**, *8*, e1327.

[22] S. Schulz, H. W. Roesky, H. J. Koch, G. M. Sheldrick, D. Stalke, A. Kuhn, *Angew. Chem. Int. Ed. Engl.* **1993**, *32*, 1729 – 1731; *Angew. Chem.* **1993**, *105*, 1828 – 1830.

[23] a) C. Dohmeier, H. Schnöckel, U. Schneider, R. Ahlrichs, C. Robl, *Angew. Chem. Int. Ed. Engl.* **1993**, *32*, 1655 – 1657; *Angew. Chem.* **1993**, *105*, 1714 – 1716; b) R. W. Schurko, I. Hung, C. L. B.

Macdonald, A. H. Cowley, *J. Am. Chem. Soc.* **2002**, *124*, 13204 – 13214; c) S.-J. Lee, P. J. Shapiro, B. Twamley, *Organometallics* **2006**, *25*, 5582 – 5586; d) M. Bochmann, D. M. Dawson, *Angew. Chem. Int. Ed. Engl.* **1996**, *35*, 2226 – 2228; *Angew. Chem.* **1996**, *108*, 2371 – 2373; e) M. Huber, A. Kurek, I. Krossing, R. Mülhaupt, H. Schnöckel, *Z. Anorg. Allg. Chem.* **2009**, *635*, 1787 – 1793.

[24] In liquid injection field desorption ionisation (LIFDI) MS, a solution of the sample is canula-transfered by suction onto the FD filament, thereby allowing inert introduction of the sample and very mild ionisation of very sensitive organometallic compounds.

[25] Topology analyses of coordination compounds containing ligands with a delocalised π-system can be challenging; see for example: a) L. J. Farrugia, C. Evans, M. Tegel, *J. Phys. Chem. A* **2006**, *110*, 7952 – 7961; b) L. J. Farrugia, C. Evans, D. Lentz, M. Roemer, *J. Am. Chem. Soc.* **2009**, *131*, 1251 – 1268.

[26] CCDC 1935771, 1935772 contain the supplementary crystallographic data for this paper. These data are provided free of charge by The Cambridge Crystallographic Data Centre.

Manuscript received: June 21, 2019
Accepted manuscript online: August 7, 2019
Version of record online: September 10, 2019

